Available online at www.sciencedirect.com
ScienceDirect
Bioelectrochemistry 69 (2006) 10 – 15
Bioelectrochemistry
www.elsevier.com/locate/bioelechem

Hemoglobin/colloidal silver nanoparticles immobilized in titania sol–gel film on glassy carbon electrode: Direct electrochemistry and electrocatalysis

Shuang Zhao, Kai Zhang, Yingying Sun, Changqing Sun *

College of Chemistry, Jilin University, Changchun, 130023, PR China

Received 6 June 2005; received in revised form 29 September 2005; accepted 29 September 2005
Available online 21 November 2005

Abstract

By vapor deposition method, both hemoglobin (Hb) and colloidal silver nanoparticles (CSNs) were entrapped in a titania sol–gel matrix on the surface of a glassy carbon electrode (GCE). CSNs could greatly enhance the electron transfer reactivity of Hb and its catalytic ability toward nitrite. Direct fast electron transfer between Hb and the GCE was achieved, and a pair of well-defined, quasi-reversible redox peaks was observed. The anodic and cathodic peak potentials are located at −0.298 V and −0.364 V (vs. Ag/AgCl), respectively. The dependence of the formal potential on solution pH indicated that the direct electron transfer reaction of Hb was a one-electron transfer coupled with a one-proton transfer reaction process. Meanwhile, the catalytic ability of Hb toward the reduction of NO_2^- was also studied. Accordingly, a NO_2^- biosensor was prepared, with a linear range from 0.2 mM to 6.0 mM and a detection limit of 34.0 μM. The apparent Michaelis–Menten constant was calculated to be 7.48 mM. Moreover, the biosensor had good long-term stability.

Keywords: Hemoglobin; Colloidal silver nanoparticles; Titania sol–gel; Direct electrochemistry; Electrocatalysis

1. Introduction

Hemoglobin (Hb), a natural macromolecular protein, has a molecular weight of 64,000–67,000 and comprises four polypeptide subunits (two α and two β subunits), each of which has an iron-bearing heme within molecularly accessible crevices and has a similar structure [1]. The physiological function of Hb is to store and transport oxygen in the blood of vertebrates. Although Hb does not function as an electron carrier in biological systems, it is considered to be an ideal model protein for the study of electron transfer of heme proteins because of its commercial availability, a known and documented structure and enzyme-like oxidative and reductive catalytic activity [2–4]. Unfortunately, it is difficult for Hb in solution to exchange electrons directly with bare solid electrodes for the following reasons. Firstly, its electroactive center is deeply buried in its electrochemically "insulated" peptide backbone; secondly, the protein would adsorb on the electrode surface, resulting in the denaturation and loss of both electrochemical and bioactivity. So different mediators and promoters are used to facilitate electron transfer for Hb [5,6]. However, direct electrochemistry of redox proteins has great significance since it establishes a model for the mechanistic study of electron exchange among proteins in biological systems and provides a foundation for fabrication of the third-generation biosensors [7]. So many methods have been employed to realize the direct electrochemistry of the proteins [8–10].

The sol–gel process provides an attractive and convenient method for the incorporation of all kinds of electroactive materials into the sol–gel matrix, including a lot of biomolecules [11,12]. The proteins in the sol–gel matrix have been reported to retain their functional characteristics to a great extent [13–15]. Recently, vapor deposition has been used as an alternative method for the formation of sol–gel films [16,17]. This novel method is more simple and practical than the traditional ones. On the other hand, there has been an increasing interest in the fabrication of the nanoparticle-based electrodes in recent years. The combination of nanomaterials and biomolecules is of considerable importance in the fields of biotechnology and bioelectrochemistry, because nanoparticles can play an important role in improving the biosensor

* Corresponding author. Tel./fax: +86 431 8499355.
E-mail address: sunchq@mail.jlu.edu.cn (C. Sun).

1567-5394/$ - see front matter © 2005 Elsevier B.V. All rights reserved.
doi:10.1016/j.bioelechem.2005.09.004

performance due to their large specific surface area, excellent conductivity and biocompatibility. Many nanoparticles have been widely used in constructing electrochemical biosensors, such as gold [18–20] and SiO_2 nanoparticles [21,22]. Although those nanoparticles have been proven to be successful for preparation of biosensors, to explore other nanoparticles, which have good stability and are easy to synthesize, is still a challenge. In this work, we attempt to combine the advantages of sol–gel technology and nanoparticles to study the direct electrochemistry and eletrocatalysis of protein. Colloidal silver nanoparticles (CSNs), which are easy to synthesize, have attracted our attention due to their quantum characteristics of small granule diameter and large specific surface area as well as their ability to quickly transfer photoinduced electrons at the surfaces of colloidal particles [23,24]. Briefly, both the Hb and CSNs were entrapped into the titania sol–gel matrix by a vapor deposition method. The immobilized Hb exhibits good direct electrochemical behavior and sensitive electrocatalytic ability to the reduction of nitrite. The performance of the biosensor was studied in detail.

2. Experimental

2.1. Reagents

Hb (from bovine red cells) was obtained from Shanghai Shenggong Co. (China) and used as received. Titanium isopropoxide was purchased from Acros. $AgNO_3$ was purchased from Beijing Chemical Reagent Co. (China). 3-Mercapto-1-propanesulfonic acid sodium salt was purchased from Aldrich. 0.1 M phosphate buffer solutions (PBS) with various pH values were prepared by mixing stock standard solutions of Na_2HPO_4 and NaH_2PO_4 and adjusting the pH values with 0.1 M H_3PO_4 or NaOH solutions. Acetate buffer solutions (0.2 M) with various pH values were prepared by mixing stock standard solutions of HA_C and NaA_C. All other chemicals were of analytical grade and were used without further purification. All solutions were made up with twice-distilled water.

2.2. Apparatus

UV–Vis spectra were recorded on a GBC Cintra 10_e UV–Visible spectrometer. The electrochemical experiments were carried out with a CHI 660A electrochemical workstation (CH Instruments, USA) with a conventional three-electrode cell. The modified or unmodified glassy carbon electrode was used as the working electrode. The Pt wire and the Ag/AgCl electrode were used as the counter and reference electrodes, respectively. All solutions were purged with high-purity nitrogen for at least 20 min prior to experiments and a nitrogen environment was then kept over the solution in the cell. Amperometric experiments were carried out in a stirred cell operated at −730 mV upon successive additions of 10 μL 0.2 M $NaNO_2$. Current–time data were recorded after a steady-state current was achieved. All experiments were performed at room temperature. Transmission electron microscopy (TEM) photographs were recorded with a Hitachi 8100 instrument at 200 kV.

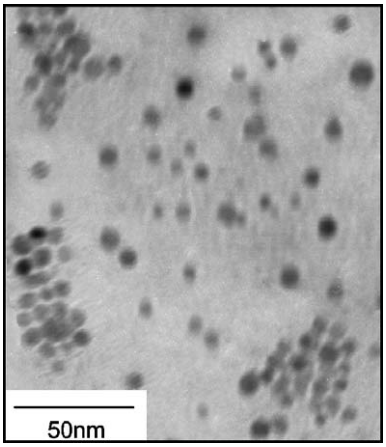

Fig. 1. TEM photograph of colloidal silver nanoparticles.

2.3. Preparation of colloidal silver nanoparticles

Mercaptosulfonic acid-capped spherical colloidal silver nanoparticles were prepared by a simple chemical reaction. A total of 2.5 mL of 0.01 M $AgNO_3$ was added to 50 mL of triply distilled water. A total of 5 mL of 0.01 M 3-mercapto-1-propanesulfonic acid sodium salt was added as stabilizer to the solution with stirring. After 10 min of mixing, 2.5 mL of 0.01 M KI was dropped into the solution slowly, yielding a green-yellow AgI colloid. A total of 20 mg of $NaBH_4$ was then added to the AgI colloidal solution, and the reaction mixture was continually stirred for about 20 min. The CSNs were finally obtained. The average nanoparticles diameter is about 8 nm measured by TEM, as shown in Fig. 1.

2.4. Preparation of the GCE/Hb–colloidal silver nanoparticles/titania sol–gel electrode

Glassy carbon electrodes (GCE, diameter of 3 mm) were polished carefully with 1.0, 0.3 and 0.05 μm alumina slurry. After rinsing thoroughly with twice-distilled water, they were sonicated in absolute ethanol and twice-distilled water for about 1 min, respectively.

For the preparation of Hb–colloidal silver nanoparticles/titania sol–gel film modified GCE (GCE/Hb–CSNs/TiO_2 Sol–Gel), Hb solution was first obtained by dissolving 2.5 mg of Hb in 1 mL of 0.2 M pH 4.8 acetate buffer solution, and the CSNs was used as prepared. Then a 10-μL mixture of Hb and colloidal silver solution (v/v = 2 : 1) was dropped onto the surface of a cleaned GCE. The electrode was then suspended vertically above titanium isopropoxide in a sealed flask kept at a constant temperature of 30 °C for 3 h. All resulting electrodes were washed with water and stored at 4 °C when not in use.

3. Results and discussion

3.1. UV–Vis absorption spectra

The position of the Soret absorption band of heme can provide information on the possible denaturation of heme protein, especially that of conformational change in the heme

group region. Film cast from Hb alone gave a Soret band at 407 nm (Fig. 2a), which was similar to the Soret band at 406 nm for native Hb in buffer. The Soret band of Hb/titania sol–gel film at 411 nm (Fig. 2b) was also very close to that in buffer. This indicated that the heme status for the entrapped Hb molecules in titania sol–gel film was similar to that in the native protein.

3.2. Direct electrochemistry of Hb

The cyclic voltammogram (CV) of GCE/Hb–CSNs/TiO_2 Sol–Gel in pH 7.0 PBS exhibited a pair of well-defined and nearly reversible redox peaks, as shown in Fig. 3a, while no peak was observed at GCE/CSNs/TiO_2 Sol–Gel (Fig. 3c). Obviously, the response of GCE/Hb–CSNs/TiO_2 Sol–Gel was attributed to the redox of the electroactive center of the immobilized Hb. The anodic peak potential (E_{pa}) and cathodic peak potential (E_{pc}) are located at −0.298 and −0.364 V, respectively, at 100 mV/s. The separation of peak potentials, ΔE_p, is 66 mV. The formal potential ($E^{0\prime}$), calculated from the average value of the anodic and cathodic peak potentials, is −0.331 V. The value of $E^{0\prime}$ is similar to that previously reported for Hb entrapping into polymer films, such as poly(vinyl sulfonate) or Eastman AQ film by Hu et al. [25,26]. It is also similar to those of other heme-containing proteins (enzymes) including myoglobin [27], horseradish peroxidase [28], and cytochrome $P450_{cam}$ [29]. According to those reported previously, the electrochemical reaction represented by Fig. 3a corresponds to the conversion of Hb–Fe(III) and Hb–Fe(II). When Hb was immobilized in titania sol–gel film without the presence of CSNs, the CV showed a small response of Hb (Fig. 3b), indicating that the titania sol–gel film was favorable to the direct electron transfer of Hb. However, the response is much smaller than that of GCE/Hb–CSNs/TiO_2 Sol–Gel. Moreover, the redox peaks were asymmetric and the reduction peak was bigger than its oxidation peak. The experimental results showed that CSNs facilitated the electron transfer of Hb due to the improvement of the microenvironment for the electron transfer of redox protein. In fact, CSNs could play the role of an efficient electron-conducting tunnel and reduce the insulating property of the protein shell for the direct electron transfer [30]. Furthermore, the strong interaction between CSNs and Hb may cause adsorbed protein to possess multiple orientations. Some of the restricted orientations may favor the direct electron transfer reaction due to the short distance between Hb and the electrode [31].

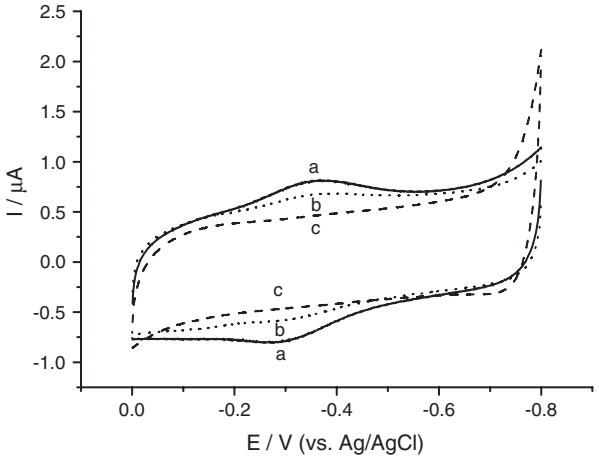

Fig. 3. Cyclic voltammograms of GCE/Hb–CSNs/TiO_2 Sol–Gel (a, solid line), GCE/Hb/TiO_2 Sol–Gel (b, dot line), and GCE/CSNs/TiO_2 Sol–Gel (c, dash line) in pH 7.0 PBS at scan rate of 100 mV/s.

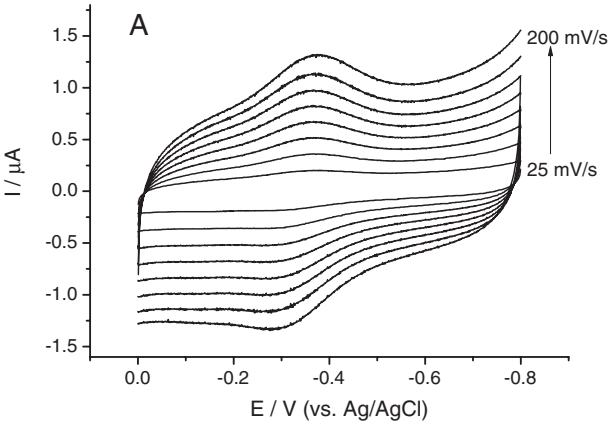

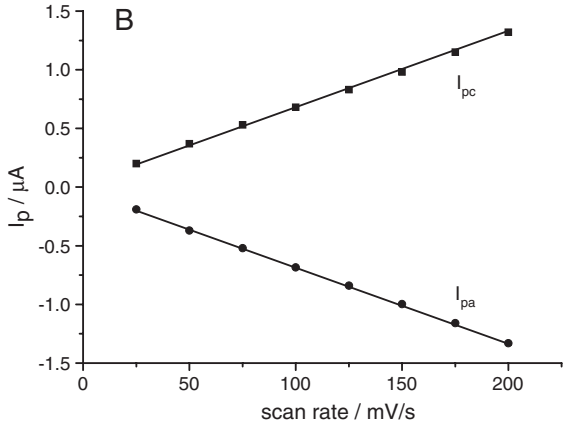

Fig. 4. (A) Cyclic voltammograms of GCE/Hb–CSNs/TiO_2 Sol–Gel in pH 7.0 PBS at scan rates of 25, 50, 75, 100, 125, 150 and 200 mV/s (from inner curve to outer curve). (B) Plot of peak current vs. scan rate.

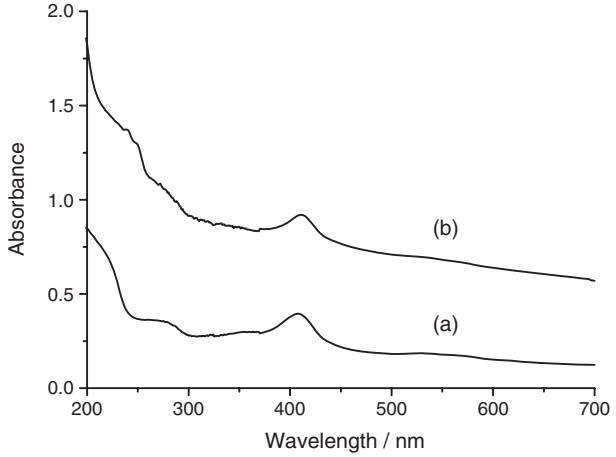

Fig. 2. UV–Vis absorption spectra of Hb (a) and Hb/titania sol–gel (b) film on quartz slides.

Fig. 4A shows the CVs of GCE/Hb–CSNs/TiO_2 Sol–Gel in pH 7.0 PBS at different scan rates. CVs of GCE/Hb–CSNs/TiO_2 Sol–Gel are almost symmetrical and the redox peak currents increased linearly with the scan rate between 25 and 200 mV/s (Fig. 4B), as expected for a thin-layer electrochemical behavior. Moreover, the cathodic peak currents were almost the same as the corresponding anodic peak currents and the peak potentials nearly did not change with increasing scan rate, indicating that all the electroactive ferric hemoglobin [Hb–Fe(III)] in the film is reduced to ferrous hemoglobin [Hb–Fe(II)] on the forward scan to negative potentials and that the Hb–Fe(II) produced is reoxidized to Hb–Fe(III) on the reverse scan.

In most cases, protein redox behavior is often significantly dependent on the pH of the external solution. CVs of GCE/Hb–CSNs/TiO_2 Sol–Gel also showed a strong dependence on pH of solutions. An increase in solution pH caused a negative shift in potentials for both reduction and oxidation peaks for the modified electrode (Fig. 5A). In addition, all changes in CV peak potentials and currents with pH were reversible between pH 5.0 and 11.0, that is, the same CV could be obtained if the electrode was transferred from a solution with a different pH to its original solution. Fig. 5B shows the effect of pH on the formal potential of the modified electrode. $E^{0\prime}$ has a linear relationship with pH from 5.0 to 11.0 with a slope of −50.0 mV/pH. This slope value is close to the theoretical value of −57.6 mV/pH at 18 °C for a reversible one-electron transfer coupled by single-proton transportation. Thus, the reaction scheme for the electrochemical reduction and oxidation of Hb can be written as follows:

$$\text{Hb} - \text{heme} - \text{Fe(III)} + \text{H}^+ + \text{e}^- \rightleftharpoons \text{Hb} - \text{heme} - \text{Fe(II)}$$

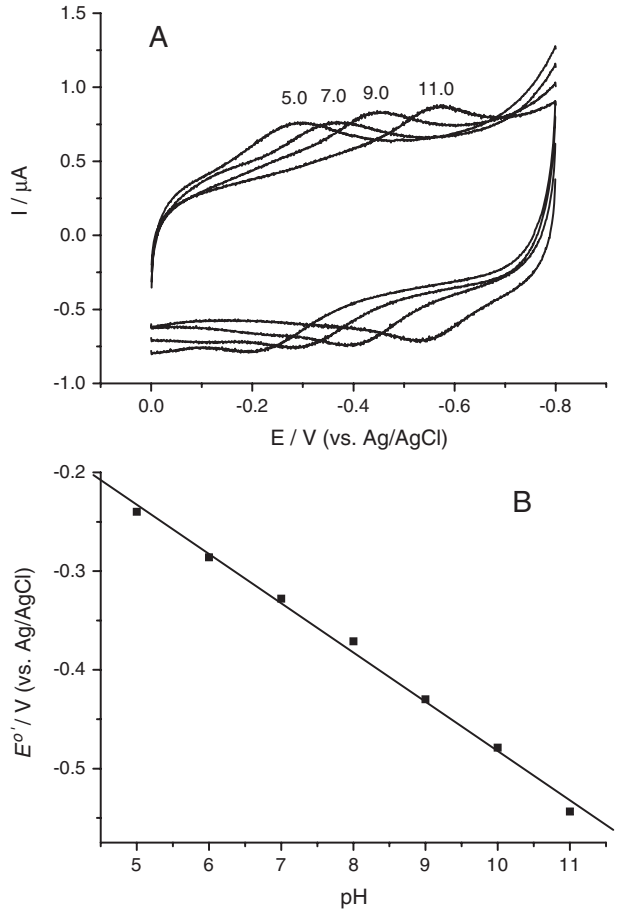

Fig. 5. (A) Cyclic voltammograms of GCE/Hb–CSNs/TiO_2 Sol–Gel at scan rate of 100 mV/s in PBS with different pH values of 5.0, 7.0, 9.0 and 11.0. (B) The linear plot of the formal potentials vs. pH.

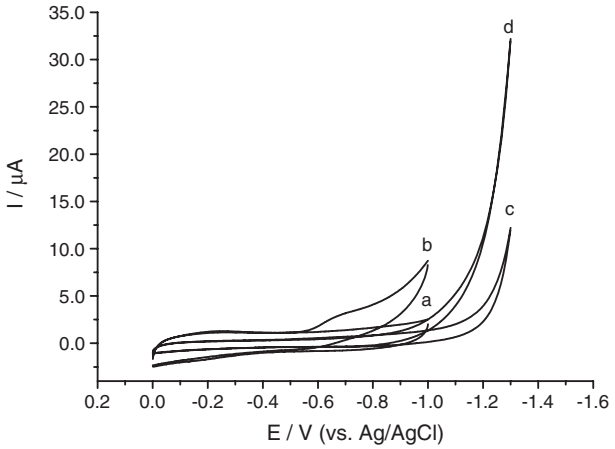

Fig. 6. Cyclic voltammograms at scan rate of 100 mV/s in pH 4.5 acetate buffers for (a) GCE/Hb–CSNs/TiO_2 Sol–Gel in the absence of NO_2^-, (b) GCE/Hb–CSNs/TiO_2 Sol–Gel in the presence of 1.0 mM NO_2^-, (c) GCE/CSNs/TiO_2 Sol–Gel in the absence of NO_2^-, and (d) GCE/CSNs/TiO_2 Sol–Gel in the presence of 1.0 mM NO_2^-.

3.3. Electrocatalytic reduction of nitrite at the GCE/Hb–CSNs/TiO_2 Sol–Gel

Nitrite exists widely in the environment, beverages, and food products as a preservative [32]. So the quantitative determination of nitrite concentrations is of rapidly increasing interest. To check the electrocatalytic ability of GCE/Hb–CSNs/TiO_2 Sol–Gel to the reduction of nitrite, CV measurements were performed (Fig. 6). When the GCE/Hb–CSNs/TiO_2 Sol–Gel was placed in 0.2 M pH 4.5 acetate buffer

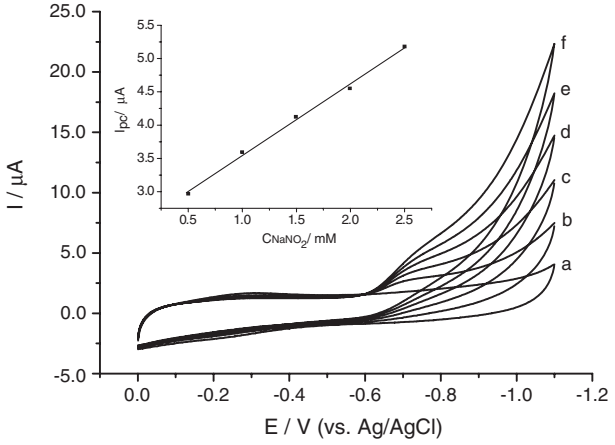

Fig. 7. Cyclic voltammograms of GCE/Hb–CSNs/TiO_2 Sol–Gel in pH 4.5 acetate buffer at scan rate of 100 mV/s. $C_{NO_2^-}$/mM: (a) 0; (b) 0.5; (c) 1.0; (d) 1.5; (e) 2.0 and (f) 2.5. Inset shows the relationship between reduction currents and the concentrations of NO_2^-. The reduction current was measured at potential of −0.70 V.

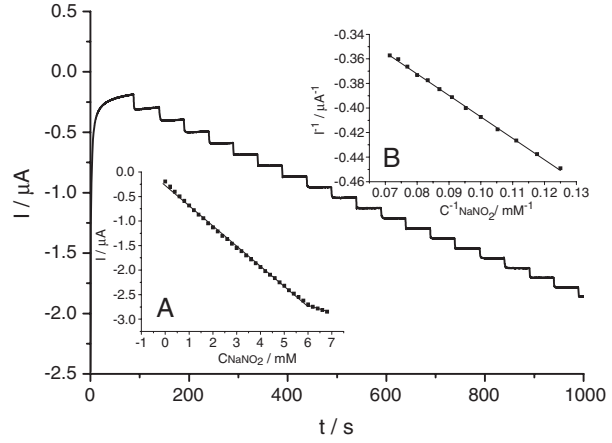

Fig. 8. Amperometric responses of GCE/Hb–CSNs/TiO_2 Sol–Gel at applied potential of −730 mV upon successive additions of 10 μL 0.2 M NO_2^- to 10.0 mL pH 4.5 acetate buffer. Inset A: linear relation between the amperometric responses and NO_2^- concentrations. Inset B: the plot of I^{-1} vs. C^{-1}.

solution containing 1.0 mM NO_2^-, a new reduction peak appeared at about −0.70 V (Fig. 6b). While the direct reduction of NO_2^- at GCE/CSNs/TiO_2 Sol–Gel was found to begin at about −1.10 V (Fig. 6d). The overpotential required for the reduction of NO_2^- was thus lowered by GCE/Hb–CSNs/TiO_2 Sol–Gel by at least 0.40 V.

Fig. 7 shows the influence of NO_2^- concentrations on the CVs of GCE/Hb–CSNs/TiO_2 Sol–Gel. The reduction peak current increases with increasing NO_2^- concentration. Good linearity is found in the plot of peak currents vs. NO_2^- concentrations (Inset in Fig. 7). The result shows that GCE/Hb–CSNs/TiO_2 Sol–Gel has potential application for quantitative determination of nitrite in solutions.

Fig. 8 shows a typical current–time plot of GCE/Hb–CSNs/TiO_2 Sol–Gel at applied potential of −730 mV upon successive additions of aliquot NO_2^- to pH 4.5 acetate buffer solution. As the NO_2^- was added into the stirring buffer solution, GCE/Hb–CSNs/TiO_2 Sol–Gel responded rapidly to the substrates and could achieve 95% of the steady-state current within 2.5 s, indicating a fast amperometric response to NO_2^- reduction. The amperometric response showed a linear relation with nitrite concentration from 0.2 mM to 6.0 mM with a correlation coefficient of −0.9991 (n=31) (inset A in Fig. 8), which is wider than the previous nitrite sensors. It has a sensitivity of −5.84 μA mM^{-1} cm^{-2} and the detection limit was estimated to be 34.0 μM at a signal-to-noise of 3. When the concentration of NO_2^- was higher than 6.0 mM, a plateau was observed, showing the characteristics of the Michaelis–Menten kinetics. The apparent Michaelis–Menten constant (K_m), a reflection of the proteinic affinity and the ratio of microscopic kinetic constants, can be obtained from the electrochemical version of the Linweaver–Burk equation [33].

$$\frac{I}{I_{ss}} = \frac{K_m}{I_{max}} \cdot \frac{1}{c} + \frac{1}{I_{max}}$$

Here, I_{ss} is the steady-state current after the addition of substrate, c is the bulk concentration of the substrate, and I_{max} is the maximum current measured under saturated substrate conditions. The K_m value of the NO_2^- sensor was found to be 7.48 mM.

3.4. Stability of the GCE/Hb–CSNs/TiO_2 Sol–Gel

The GCE/Hb–CSNs/TiO_2 Sol–Gel is fairly stable. It could remain in the direct electrochemistry of the immobilized Hb at constant current values upon continuous CV sweep at the potential range from −0.8 V to 0 V at scan rate of 100 mV/s. After the modified electrode was stored at 4 °C for 1 week, the currents for the direct electron transfer of Hb and the responses to NO_2^- have no change. Even after stored for 1 month, the reduction current of NO_2^- still remains 95% of its initial value. The high stability originates from the essence of the preparing method. This method combines the advantageous features of both CSNs and sol–gel technology. Just as previous illumination, the above two aspects are helpful to remain the bioactivity of Hb and prevent it from leaking out of the sol–gel film.

4. Conclusions

In this paper, we fabricated a biosensor by entrapping Hb/CSNs in titania sol–gel matrix on GCE by a vapor deposition method. This novel method is simple, convenient and versatile. The presence of CSNs has greatly enhanced the direct electron transfer of Hb. The resulting biosensor exhibited excellent electrocatalytic response to the reduction of nitrite and can be used as an amperometric sensor for the determination of nitrite. In addition, the biosensor also possesses high sensitivity and good chemical and mechanical stability.

Acknowledgements

This work was supported by the Major State Basic Research Development Program (G2000078102), Educational Ministry (20020183007), National Natural Science Foundation (20175007) of China, and Key Laboratory for Supramolecular Structure and Materials of Ministry of Education, Jilin University.

References

[1] C. Lei, U. Wollenberger, N. Bistolas, A. Guiseppi-Elis, F.W. Scheller, Electron transfer of hemoglobin at electrodes modified with colloidal clay nanoparticle, Anal. Bioanal. Chem. 372 (2002) 235–239.
[2] J.F. Rusling, Enzyme bioelectrochemistry in cast biomembrane-like films, Acc. Chem. Res. 31 (1998) 363–369.
[3] X. Chen, N. Hu, Y. Zeng, J.F. Rusling, J. Yang, Ordered electrochemically active films of hemoglobin, didodecyldimethylammonium ions, and clay, Langmuir 15 (1999) 7022–7030.
[4] C. Fan, H. Wang, S. Sun, D. Zhu, G. Wagner, G. Li, Electron-transfer reactivity and enzymatic activity of hemoglobin in a SP sephadex membrane, Anal. Chem. 73 (2001) 2850–2854.
[5] J. Ye, R.P. Baldwin, Catalytic reduction of myoglobin and hemoglobin at chemically modified electrodes containing methylene blue, Anal. Chem. 60 (1988) 2263–2268.
[6] M. Li, N. Li, Z. Gu, X. Zhou, Y. Sun, Y. Wu, Electrocatalysis by a C_{60}-γ-cyclodextrin (1:2) and nafion chemically modified electrode of hemoglobin, Anal. Chim. Acta 356 (1997) 225–229.

[7] L. Gorton, A. lindgren, T. Larsson, F.D. Munteanu, T. Ruzgas, I. Gazaryan, Direct electron transfer between heme-containing enzymes and electrodes as basis for third generation biosensors, Anal. Chim. Acta 400 (1999) 91–108.
[8] C. Cai, J. Chen, Direct electron transfer and bioelectrocatalysis of hemoglobin at a carbon nanotube electrode, Anal. Biochem. 325 (2004) 285–292.
[9] Y. Zhang, P. He, N. Hu, Horseradish peroxidase immobilized in TiO_2 nanoparticle films on pyrolytic graphite electrodes: direct electrochemistry and bioelectrocatalysis, Electrochim. Acta 49 (2004) 1981–1988.
[10] L. Shem, R. Huang, N. Hu, Myoglobin in polyacrylamide hydrogel films: direct electrochemistry and electrochemical catalysis, Talanta 56 (2002) 1131–1139.
[11] R. Makote, M.M. Collinson, Template recognition in inorganic–organic hybrid films prepared by the sol–gel process, Chem. Mater. 10 (1998) 2440–2445.
[12] T. Yao, K. Takashima, Amperometric biosensor with a composite membrane of sol–gel derived enzyme film and electrochemically generated poly(1,2-diaminobenzene) film, Biosens. Bioelectron. 13 (1998) 67–73.
[13] D. Avnir, Organic chemistry within ceramic matrixes: doped sol–gel materials, Acc. Chem. Res. 28 (1995) 328–334.
[14] T.K. Das, I. Khan, D.L. Rousseau, J.M. Friedman, Preservation of the native structure in myoglobin at low pH by sol–gel encapsulation, J. Am. Chem. Soc. 120 (1998) 10268–10269.
[15] Q. Ji, C.R. Lloyd, W.R. Ellis Jr., E.M. Eyring, Sol–gel-encapsulated heme proteins. Evidence for CO_2 adducts, J. Am. Chem. Soc. 120 (1998) 221–222.
[16] J. Yu, H. Ju, Preparation of porous titania sol–gel matrix for immobilization of horseradish peroxidase by a vapor deposition method, Anal. Chem. 74 (2002) 3579–3583.
[17] J. Yu, H. Ju, Amperometric biosensor for hydrogen peroxide based on hemoglobin entrapped in titania sol–gel film, Anal. Chim. Acta 486 (2003) 209–216.
[18] L. Wang, E. Wang, Direct electron transfer between cytochrome *c* and a gold nanoparticles modified electrode, Electrochem. Commun. 6 (2004) 19–54.
[19] J. Zhao, R.W. Stonchuerner, J.P. O'Daly, A.L. Crumbliss, Direct electron transfer at horseradish peroxidase-colloidal gold modified electrodes, J. Electroanal. Chem. 327 (1992) 109–119.
[20] H. Gu, A. Yu, H. Chen, Direct electron transfer and characterization of hemoglobin immobilized on a Au colloidal-cysteamine-modified gold electrode, J. Electroanal. Chem. 516 (2001) 119–126.
[21] L.R. Hilliard, X. Zhao, W. Tan, Immobilization of oligonucleotides onto silica nanoparticles for DNA hybridization studies, Anal. Chim. Acta 470 (2002) 51–56.
[22] M. Qhobosheane, S. Santra, P. Zhang, W. Tan, Biochemically functionalized silica nanoparticles, Analyst 126 (2001) 1274–1278.
[23] J. Zheng, G. Chumanov, T.M. Cotton, Photoinduced electron transfer at the surface of nanosized silver particles as monitored by EPR spectroscopy, Chem. Phys. Lett. 349 (2001) 367–370.
[24] T. Liu, J. Zhong, X. Gan, C. Fan, G. Li, N. Matsuda, Wiring electrons of cytochrome *c* with silver nanoparticles in layered films, ChemPhysChem 4 (2003) 1364–1366.
[25] L. Wang, N. Hu, Direct electrochemistry of hemoglobin in layer-by-layer films with poly(vinyl sulfonate) grown on pyrolytic graphite electrodes, Bioelectrochemistry 53 (2001) 205–212.
[26] J. Yang, N. Hu, J.F. Rusling, Enhanced electron transfer for hemoglobin in poly(ester sulfonic acid) films on pyrolytic graphite electrodes, J. Electroanal. Chem. 463 (1999) 53–62.
[27] H. Ma, N. Hu, J.F. Rusling, Electroactive myoglobin films grown layer-by-layer with poly(styrenesulfonate) on pyrolytic graphite electrodes, Langmuir 16 (1999) 4969–4975.
[28] S. Liu, H. Ju, Renewable reagentless hydrogen peroxide sensor based on direct electron transfer of horseradish peroxidase immobilized on colloidal gold-modified electrode, Anal. Biochem. 307 (2002) 110–116.
[29] Z. Zhang, A.-E.F. Nassar, Z. Lu, J.B. Schenkman, J.F. Rusling, Direct electron injection from electrodes to cytochrome in P450cam in biomembrane-like films, Faraday Trans. 93 (1997) 1769–1774.
[30] K.R. Brown, A.P. Fox, M.J. Natan, Morphology-dependent electrochemistry of cytochrome *c* at Au colloid-modified SnO_2 electrodes, J. Am. Chem. Soc. 118 (1996) 1154–1157.
[31] Y. Xiao, H. Ju, H. Chen, Direct electrochemistry of horseradish peroxidase immobilized on a colloid/cysteamine-modified gold electrode, Anal. Biochem. 278 (2000) 22–28.
[32] J. Davis, R.G. Compton, Sonoelectrochemically enhanced nitrite detection, Anal. Chim. Acta 404 (2000) 241–247.
[33] R.A. Kamin, G.S. Wilson, Rotating ring-dish enzyme electrode for biocatalysis kinetic studies and characterization of the immobilized enzyme layer, Anal. Chem. 52 (1980) 1198–1205.